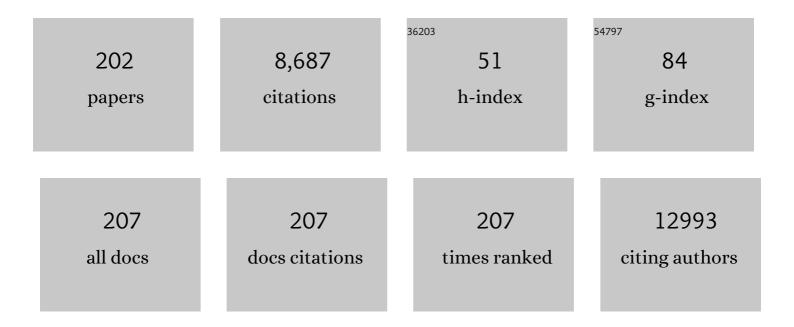
## Xiang-Heng Xiao

List of Publications by Year in descending order

Source: https://exaly.com/author-pdf/1969688/publications.pdf Version: 2024-02-01



#	Article	IF	CITATIONS
1	High Mobility MoS <sub>2</sub> Transistor with Low Schottky Barrier Contact by Using Atomic Thick hâ€BN as a Tunneling Layer. Advanced Materials, 2016, 28, 8302-8308.	11.1	398
2	Electron density modulation of NiCo2S4 nanowires by nitrogen incorporation for highly efficient hydrogen evolution catalysis. Nature Communications, 2018, 9, 1425.	5.8	356
3	Interface Engineering for Highâ€Performance Topâ€Gated MoS <sub>2</sub> Fieldâ€Effect Transistors. Advanced Materials, 2014, 26, 6255-6261.	11.1	272
4	Breaking the Currentâ€Retention Dilemma in Cationâ€Based Resistive Switching Devices Utilizing Graphene with Controlled Defects. Advanced Materials, 2018, 30, e1705193.	11.1	190
5	3D Flowerlike α-Fe <sub>2</sub> 0 <sub>3</sub> @TiO <sub>2</sub> Core–Shell Nanostructures: General Synthesis and Enhanced Photocatalytic Performance. ACS Sustainable Chemistry and Engineering, 2015, 3, 2975-2984.	3.2	184
6	Plasmon-driven reaction controlled by the number of graphene layers and localized surface plasmon distribution during optical excitation. Light: Science and Applications, 2015, 4, e342-e342.	7.7	178
7	Controllable Synthesis, Magnetic Properties, and Enhanced Photocatalytic Activity of Spindlelike Mesoporous α-Fe <sub>2</sub> O <sub>3</sub> /ZnO Core–Shell Heterostructures. ACS Applied Materials & Interfaces, 2012, 4, 3602-3609.	4.0	168
8	Hydrogen gas sensor based on metal oxide nanoparticles decorated graphene transistor. Nanoscale, 2015, 7, 10078-10084.	2.8	163
9	Significantly Enhanced Visible Light Photoelectrochemical Activity in TiO <sub>2</sub> Nanowire Arrays by Nitrogen Implantation. Nano Letters, 2015, 15, 4692-4698.	4.5	159
10	Volumeâ€Enhanced Raman Scattering Detection of Viruses. Small, 2019, 15, e1805516.	5.2	150
11	Active Electron Density Modulation of Co <sub>3</sub> O <sub>4</sub> â€Based Catalysts Enhances their Oxygen Evolution Performance. Angewandte Chemie - International Edition, 2020, 59, 6929-6935.	7.2	148
12	Confining Cation Injection to Enhance CBRAM Performance by Nanopore Graphene Layer. Small, 2017, 13, 1603948.	5.2	147
13	A one-pot route to the synthesis of alloyed Cu/Ag bimetallic nanoparticles with different mass ratios for catalytic reduction of 4-nitrophenol. Journal of Materials Chemistry A, 2015, 3, 3450-3455.	5.2	145
14	Rational Design of Sub-Parts per Million Specific Gas Sensors Array Based on Metal Nanoparticles Decorated Nanowire Enhancement-Mode Transistors. Nano Letters, 2013, 13, 3287-3292.	4.5	132
15	Large-Scale and Controlled Synthesis of Iron Oxide Magnetic Short Nanotubes: Shape Evolution, Growth Mechanism, and Magnetic Properties. Journal of Physical Chemistry C, 2010, 114, 16092-16103.	1.5	121
16	Ultrasensitive SERS performance in 3D "sunflower-like―nanoarrays decorated with Ag nanoparticles. Nanoscale, 2017, 9, 3114-3120.	2.8	118
17	Synthesis and Magnetic Properties of Maghemite (Î <sup>3</sup> -Fe2O3) Short-Nanotubes. Nanoscale Research Letters, 2010, 5, 1474-1479.	3.1	113
18	Fe-Doped BiOCl Nanosheets with Light-Switchable Oxygen Vacancies for Photocatalytic Nitrogen Fixation. ACS Applied Energy Materials, 2019, 2, 8394-8398.	2.5	109

#	Article	IF	CITATIONS
19	Fully Tensile Strained Pd <sub>3</sub> Pb/Pd Tetragonal Nanosheets Enhance Oxygen Reduction Catalysis. Nano Letters, 2019, 19, 1336-1342.	4.5	109
20	Low-Cost, Disposable, Flexible and Highly Reproducible Screen Printed SERS Substrates for the Detection of Various Chemicals. Scientific Reports, 2015, 5, 10208.	1.6	106
21	Transparent, Highâ€Performance Thinâ€Film Transistors with an InGaZnO/Alignedâ€5nO <sub>2</sub> â€Nanowire Composite and their Application in Photodetectors. Advanced Materials, 2014, 26, 7399-7404.	11.1	104
22	Floating Gate Memory-based Monolayer MoS <sub>2</sub> Transistor with Metal Nanocrystals Embedded in the Gate Dielectrics. Small, 2015, 11, 208-213.	5.2	102
23	Beehive-Inspired Macroporous SERS Probe for Cancer Detection through Capturing and Analyzing Exosomes in Plasma. ACS Applied Materials & Interfaces, 2020, 12, 5136-5146.	4.0	102
24	Ultrasensitive SERS Substrate Integrated with Uniform Subnanometer Scale "Hot Spots―Created by a Graphene Spacer for the Detection of Mercury Ions. Small, 2017, 13, 1603347.	5.2	101
25	Sizeâ€Dependent Nickelâ€Based Electrocatalysts for Selective CO <sub>2</sub> Reduction. Angewandte Chemie - International Edition, 2020, 59, 18572-18577.	7.2	100
26	Forceâ€Induced Turnâ€On Persistent Roomâ€Temperature Phosphorescence in Purely Organic Luminogen. Angewandte Chemie - International Edition, 2021, 60, 12335-12340.	7.2	98
27	Mechanism of the enhancement and quenching of ZnO photoluminescence by ZnO-Ag coupling. Europhysics Letters, 2011, 93, 57009.	0.7	96
28	Sub-ppb detection of acetone using Au-modified flower-like hierarchical ZnO structures. Sensors and Actuators B: Chemical, 2015, 219, 209-217.	4.0	95
29	Facile method to synthesize magnetic iron oxides/TiO2 hybrid nanoparticles and their photodegradation application of methylene blue. Nanoscale Research Letters, 2011, 6, 533.	3.1	90
30	Controlled synthesis of magnetic iron oxides@SnO2 quasi-hollow core–shell heterostructures: formation mechanism, and enhanced photocatalytic activity. Nanoscale, 2011, 3, 4676.	2.8	87
31	Ag-decorated ultra-thin porous single-crystalline ZnO nanosheets prepared by sunlight induced solvent reduction and their highly sensitive detection of ethanol. Sensors and Actuators B: Chemical, 2015, 209, 975-982.	4.0	87
32	Controllable Electrical Properties of Metal-Doped In <sub>2</sub> O <sub>3</sub> Nanowires for High-Performance Enhancement-Mode Transistors. ACS Nano, 2013, 7, 804-810.	7.3	85
33	Rational Design of Amorphous Indium Zinc Oxide/Carbon Nanotube Hybrid Film for Unique Performance Transistors. Nano Letters, 2012, 12, 3596-3601.	4.5	83
34	Tube-Like Ternary α-Fe <sub>2</sub> O <sub>3</sub> @SnO <sub>2</sub> @Cu <sub>2</sub> O Sandwich Heterostructures: Synthesis and Enhanced Photocatalytic Properties. ACS Applied Materials & Interfaces, 2014, 6, 13088-13097.	4.0	81
35	The "Midas Touch―Transformation of TiO <sub>2</sub> Nanowire Arrays during Visible Light Photoelectrochemical Performance by Carbon/Nitrogen Coimplantation. Advanced Energy Materials, 2018, 8, 1800165.	10.2	77
36	Rational Design of ZnO:H/ZnO Bilayer Structure for High-Performance Thin-Film Transistors. ACS Applied Materials & Interfaces, 2016, 8, 7862-7868.	4.0	76

#	Article	IF	CITATIONS
37	Near-Infrared Light-Triggered Porous AuPd Alloy Nanoparticles To Produce Mild Localized Heat To Accelerate Bone Regeneration. Journal of Physical Chemistry Letters, 2019, 10, 4185-4191.	2.1	76
38	Integration of Highâ€ <i>k</i> Oxide on MoS <sub>2</sub> by Using Ozone Pretreatment for Highâ€Performance MoS <sub>2</sub> Topâ€Gated Transistor with Thicknessâ€Dependent Carrier Scattering Investigation. Small, 2015, 11, 5932-5938.	5.2	74
39	WSe2/GeSe heterojunction photodiode with giant gate tunability. Nano Energy, 2018, 49, 103-108.	8.2	73
40	A Review of Recent Applications of Ion Beam Techniques on Nanomaterial Surface Modification: Design of Nanostructures and Energy Harvesting. Small, 2019, 15, e1901820.	5.2	72
41	SiO2–Ag–SiO2–TiO2 multi-shell structures: plasmon enhanced photocatalysts with wide-spectral-response. Journal of Materials Chemistry A, 2013, 1, 13128.	5.2	71
42	Template and Silica Interlayer Tailorable Synthesis of Spindle-like Multilayer α-Fe <sub>2</sub> O <sub>3</sub> /Ag/SnO <sub>2</sub> Ternary Hybrid Architectures and Their Enhanced Photocatalytic Activity. ACS Applied Materials & Interfaces, 2014, 6, 1113-1124.	4.0	67
43	Preparation and characterization of spindle-like Fe3O4 mesoporous nanoparticles. Nanoscale Research Letters, 2011, 6, 89.	3.1	66
44	Wetting properties and SERS applications of ZnO/Ag nanowire arrays patterned by a screen printing method. Journal of Materials Chemistry C, 2016, 4, 6371-6379.	2.7	65
45	Exploring Bi <sub>2</sub> Te <sub>3</sub> Nanoplates as Versatile Catalysts for Electrochemical Reduction of Small Molecules. Advanced Materials, 2020, 32, e1906477.	11.1	65
46	Scalable Integration of Indium Zinc Oxide/Photosensitiveâ€Nanowire Composite Thinâ€Film Transistors for Transparent Multicolor Photodetectors Array. Advanced Materials, 2014, 26, 2919-2924.	11.1	62
47	Shape-controlled iron oxide nanocrystals: synthesis, magnetic properties and energy conversion applications. CrystEngComm, 2016, 18, 6303-6326.	1.3	61
48	Surfaceâ€Regulated Rhodium–Antimony Nanorods for Nitrogen Fixation. Angewandte Chemie - International Edition, 2020, 59, 8066-8071.	7.2	58
49	Controlled Synthesis of Monodisperse Subâ€100â€nm Hollow SnO <sub>2</sub> Nanospheres: A Template― and Surfactantâ€Free Solutionâ€Phase Route, the Growth Mechanism, Optical Properties, and Application as a Photocatalyst. Chemistry - A European Journal, 2011, 17, 9708-9719.	1.7	57
50	Controllable synthesis of recyclable core–shell γ-Fe2O3@SnO2 hollow nanoparticles with enhanced photocatalytic and gas sensing properties. Physical Chemistry Chemical Physics, 2013, 15, 8228.	1.3	57
51	Optimizing Hydrogen Adsorption by d–d Orbital Modulation for Efficient Hydrogen Evolution Catalysis. Advanced Energy Materials, 2022, 12, .	10.2	57
52	Greatly reduced leakage current in BiFeO3thin film by oxygen ion implantation. Journal Physics D: Applied Physics, 2007, 40, 5775-5777.	1.3	51
53	Non-centrosymmetric Au–SnO2 hybrid nanostructures with strong localization of plasmonic for enhanced photocatalysis application. Nanoscale, 2013, 5, 5628.	2.8	51
54	Preparation of M@BiFeO <sub>3</sub> Nanocomposites (MÂ=ÂAg, Au) Bowl Arrays with Enhanced Visible Light Photocatalytic Activity. Journal of the American Ceramic Society, 2015, 98, 2255-2263.	1.9	50

#	Article	IF	CITATIONS
55	Oxygen vacancies enable the visible light photoactivity of chromium-implanted TiO2 nanowires. Journal of Energy Chemistry, 2021, 55, 154-161.	7.1	50
56	Significant Radiation Tolerance and Moderate Reduction in Thermal Transport of a Tungsten Nanofilm by Inserting Monolayer Graphene. Advanced Materials, 2017, 29, 1604623.	11.1	49
57	<i>In situ</i> Oxidation and Self-Assembly Synthesis of Dumbbell-like α-Fe <sub>2</sub> O <sub>3</sub> /Ag/AgX (X = Cl, Br, I) Heterostructures with Enhanced Photocatalytic Properties. ACS Sustainable Chemistry and Engineering, 2016, 4, 1521-1530.	3.2	48
58	Size effects of Ag nanoparticles on plasmon-induced enhancement of photocatalysis of Ag-α-Fe2O3 nanocomposites. Journal of Colloid and Interface Science, 2014, 427, 29-34.	5.0	46
59	Oxygen Vacancyâ€induced Electron Density Tuning of Fe <sub>3</sub> O <sub>4</sub> for Enhanced Oxygen Evolution Catalysis. Energy and Environmental Materials, 2021, 4, 392-398.	7.3	45
60	In situRaman scattering study on a controllable plasmon-driven surface catalysis reaction on Ag nanoparticle arrays. Nanotechnology, 2012, 23, 335701.	1.3	44
61	One-Pot Reaction and Subsequent Annealing to Synthesis Hollow Spherical Magnetite and Maghemite Nanocages. Nanoscale Research Letters, 2009, 4, 926-931.	3.1	43
62	Enhanced photocatalysis by coupling of anatase TiO2 film to triangular Ag nanoparticle island. Nanoscale Research Letters, 2012, 7, 239.	3.1	43
63	Improved Thermal Stability of Graphene-Veiled Noble Metal Nanoarrays as Recyclable SERS Substrates. ACS Applied Materials & Interfaces, 2017, 9, 40726-40733.	4.0	43
64	Recent progress in perovskite-based photodetectors: the design of materials and structures. Advances in Physics: X, 2019, 4, 1592709.	1.5	42
65	Anisotropic Lowâ€Dimensional Materials for Polarizationâ€5ensitive Photodetectors: From Materials to Devices. Advanced Optical Materials, 2022, 10, .	3.6	42
66	Sideâ€Gated In <sub>2</sub> O <sub>3</sub> Nanowire Ferroelectric FETs for Highâ€Performance Nonvolatile Memory Applications. Advanced Science, 2016, 3, 1600078.	5.6	41
67	Springtailâ€Inspired Superamphiphobic Ordered Nanohoodoo Arrays with Quasiâ€Doubly Reentrant Structures. Small, 2020, 16, e2000779.	5.2	41
68	Large-area, well-ordered, uniform-sized bowtie nanoantenna arrays for surface enhanced Raman scattering substrate with ultra-sensitive detection. Applied Physics Letters, 2013, 103, .	1.5	39
69	Efficient enhancement of hydrogen production by Ag/Cu2O/ZnO tandem triple-junction photoelectrochemical cell. Applied Physics Letters, 2015, 106, .	1.5	39
70	Efficiency enhancements in Ag nanoparticles-SiO2-TiO2 sandwiched structure via plasmonic effect-enhanced light capturing. Nanoscale Research Letters, 2013, 8, 73.	3.1	38
71	Anchoring of Ag <sub>6</sub> Si <sub>2</sub> O <sub>7</sub> nanoparticles on α-Fe <sub>2</sub> O <sub>3</sub> short nanotubes as a Z-scheme photocatalyst for improving their photocatalytic performances. Dalton Transactions, 2016, 45, 12745-12755.	1.6	38
72	Advanced Catalysts Derived from Compositionâ€Segregated Platinum–Nickel Nanostructures: New Opportunities and Challenges. Advanced Functional Materials, 2019, 29, 1808161.	7.8	38

#	Article	IF	CITATIONS
73	Performance Limits of the Selfâ€Aligned Nanowire Topâ€Gated MoS <sub>2</sub> Transistors. Advanced Functional Materials, 2017, 27, 1602250.	7.8	37
74	Engineering embedded metal nanoparticles with ion beam technology. Applied Physics A: Materials Science and Processing, 2009, 96, 317-325.	1.1	36
75	Active Electron Density Modulation of Co <sub>3</sub> O <sub>4</sub> â€Based Catalysts Enhances their Oxygen Evolution Performance. Angewandte Chemie, 2020, 132, 6996-7002.	1.6	34
76	Enhanced radiation tolerance in nitride multilayered nanofilms with small period-thicknesses. Applied Physics Letters, 2012, 101, .	1.5	32
77	Ag Nanoparticles Located on Three-Dimensional Pine Tree-Like Hierarchical TiO2 Nanotube Array Films as High-Efficiency Plasmonic Photocatalysts. Nanoscale Research Letters, 2017, 12, 54.	3.1	32
78	Precise Modulation of Gold Nanorods for Protecting against Malignant Ventricular Arrhythmias via Nearâ€Infrared Neuromodulation. Advanced Functional Materials, 2019, 29, 1902128.	7.8	31
79	Obviously Angular, Cuboid-Shaped TiO2 Nanowire Arrays Decorated with Ag Nanoparticle as Ultrasensitive 3D Surface-Enhanced Raman Scattering Substrates. Journal of Physical Chemistry C, 2014, 118, 22711-22718.	1.5	30
80	Metal ion-mediated synthesis and shape-dependent magnetic properties of single-crystalline α-Fe <sub>2</sub> O <sub>3</sub> nanoparticles. CrystEngComm, 2014, 16, 5566-5572.	1.3	30
81	Sizeâ€Dependent Nickelâ€Based Electrocatalysts for Selective CO <sub>2</sub> Reduction. Angewandte Chemie, 2020, 132, 18731-18736.	1.6	30
82	Third-order nonlinearity in Ag-nanoparticles embedded 56GeS2–24Ga2S3–20KBr chalcohalide glasses. Journal of Non-Crystalline Solids, 2011, 357, 2320-2323.	1.5	28
83	Polymer‣upported Bimetallic Ag@AgAu Nanocomposites: Synthesis and Catalytic Properties. Chemistry - an Asian Journal, 2012, 7, 1781-1788.	1.7	28
84	Characterization of DC reactive magnetron sputtered NiO films using spectroscopic ellipsometry. Applied Surface Science, 2011, 257, 5908-5912.	3.1	27
85	Design of wafer-scale uniform Au nanotip array by ion irradiation for enhanced single conductive filament resistive switching. Nano Energy, 2020, 67, 104213.	8.2	26
86	Manipulating Coordination Structures of Mixed-Valence Copper Single Atoms on 1T-MoS <sub>2</sub> for Efficient Hydrogen Evolution. ACS Catalysis, 2022, 12, 7687-7695.	5.5	26
87	Carbon and silica interlayer influence for the photocatalytic performances of spindle-like α-Fe 2 O 3 /Bi 2 O 3 p – n heterostructures. Materials Science in Semiconductor Processing, 2016, 41, 411-419.	1.9	25
88	Forceâ€Induced Turnâ€On Persistent Roomâ€Temperature Phosphorescence in Purely Organic Luminogen. Angewandte Chemie, 2021, 133, 12443-12448.	1.6	24
89	Enhancement of third-order nonlinearity in Ag-nanoparticles-contained chalcohalide glasses. Journal of Nanoparticle Research, 2011, 13, 3693-3697.	0.8	23
90	Anion-mediated synthesis of monodisperse silver nanoparticles useful for screen printing of high-conductivity patterns on flexible substrates for printed electronics. RSC Advances, 2015, 5, 9783-9791.	1.7	23

6

#	Article	IF	CITATIONS
91	Monolayer graphene on nanostructured Ag for enhancement of surface-enhanced Raman scattering stable platform. Nanotechnology, 2015, 26, 125603.	1.3	23
92	Design of Enhanced Catalysts by Coupling of Noble Metals (Au,Ag) with Semiconductor SnO <sub>2</sub> for Catalytic Reduction of 4â€Nitrophenol. Particle and Particle Systems Characterization, 2016, 33, 212-220.	1.2	23
93	Catalytic Application and Mechanism Studies of Argentic Chloride Coupled Ag/Au Hollow Heterostructures: Considering the Interface Between Ag/Au Bimetals. Nanoscale Research Letters, 2019, 14, 35.	3.1	23
94	Flammable gases produced by TiO2 nanoparticles under magnetic stirring in water. Friction, 2022, 10, 1127-1133.	3.4	23
95	Strong Penetrationâ€Induced Effective Photothermal Therapy by Exosomeâ€Mediated Black Phosphorus Quantum Dots. Small, 2021, 17, e2104585.	5.2	23
96	High-Mobility Solution-Processed Amorphous Indium Zinc \$hbox{Oxide/In}_{2}hbox{O}_{3} Nanocrystal Hybrid Thin-Film Transistor. IEEE Electron Device Letters, 2013, 34, 72-74.	2.2	22
97	Micro–Nanosized Nontraditional Evaporated Structures Based on Closely Packed Monolayer Binary Colloidal Crystals and Their Fine Structure Enhanced Properties. Journal of Physical Chemistry C, 2014, 118, 20521-20528.	1.5	22
98	Tube-like α-Fe <sub>2</sub> 0 <sub>3</sub> @Ag/AgCl heterostructure: controllable synthesis and enhanced plasmonic photocatalytic activity. RSC Advances, 2015, 5, 61239-61248.	1.7	22
99	Synthesis and optical properties of gold nanorods with controllable morphology. Journal of Physics Condensed Matter, 2016, 28, 434002.	0.7	22
100	Ion implantation inducing nanovoids characterized by TEM and STEM. Solid State Communications, 2006, 137, 362-365.	0.9	21
101	A Comparative Study of the Magnetic Behavior of Single and Tubular Clustered Magnetite Nanoparticles. Journal of Low Temperature Physics, 2012, 168, 306-313.	0.6	21
102	"Rings of saturn-like―nanoarrays with high number density of hot spots for surface-enhanced Raman scattering. Applied Physics Letters, 2014, 105, 033515.	1.5	21
103	Competitive Reaction Pathway for Siteâ€Selective Conjugation of Raman Dyes to Hotspots on Gold Nanorods for Greatly Enhanced SERS Performance. Small, 2014, 10, 4012-4019.	5.2	21
104	The different roles of contact materials between oxidation interlayer and doping effect for high performance ZnO thin film transistors. Applied Physics Letters, 2015, 106, 051607.	1.5	21
105	Irradiation-induced TiO2 nanorods for photoelectrochemical hydrogen production. International Journal of Hydrogen Energy, 2015, 40, 5034-5041.	3.8	21
106	Design of high-performance memristor cell using W-implanted SiO2 films. Applied Physics Letters, 2016, 108, .	1.5	21
107	The Study for Solution-Processed Alkali Metal-Doped Indium–Zinc Oxide Thin-Film Transistors. IEEE Electron Device Letters, 2016, 37, 50-52.	2.2	21
108	Ultrasensitive Au Nanooctahedron Micropinball Sensor for Mercury Ions. ACS Applied Materials & Interfaces, 2018, 10, 25737-25743.	4.0	21

#	Article	IF	CITATIONS
109	Enhanced and polarization dependence of surface-enhanced Raman scattering in silver nanoparticle array-nanowire systems. Applied Physics Letters, 2013, 102, 163108.	1.5	20
110	Modulating the threshold voltage of oxide nanowire field-effect transistors by a Ga+ ion beam. Nano Research, 2014, 7, 1691-1698.	5.8	20
111	Anionic Dopant Delocalization through pâ€Band Modulation to Endow Metal Oxides with Enhanced Visibleâ€Light Photoactivity. Angewandte Chemie - International Edition, 2019, 58, 16660-16667.	7.2	20
112	Rational design of ordered Pd–Pb nanocubes as highly active, selective and durable catalysts for solvent-free benzyl alcohol oxidation. Nanoscale, 2019, 11, 5145-5150.	2.8	20
113	Uniform, Fast, and Reliable Li <sub>x</sub> SiO <sub>y</sub> -Based Resistive Switching Memory. IEEE Electron Device Letters, 2019, 40, 554-557.	2.2	20
114	Ultrastable Laurionite Spontaneously Encapsulates Reduced-dimensional Lead Halide Perovskites. Nano Letters, 2020, 20, 2316-2325.	4.5	20
115	Controllable synthesis and catalysis application of hierarchical PS/Au core–shell nanocomposites. Journal of Colloid and Interface Science, 2012, 387, 47-55.	5.0	19
116	In situ TEM observation of helium bubble evolution in V/Ag multilayer during annealing. Journal of Nuclear Materials, 2015, 467, 537-543.	1.3	19
117	Formation of aligned silver nanoparticles by ion implantation. Materials Letters, 2007, 61, 4435-4437.	1.3	18
118	Modified in situ and self-catalytic growth method for fabrication of Ag-coated nanocomposites with tailorable optical properties. Journal of Nanoparticle Research, 2012, 14, 1.	0.8	18
119	Enhanced radiation tolerance of nanochannel V films through defects release. Nuclear Instruments & Methods in Physics Research B, 2014, 334, 1-7.	0.6	18
120	Solar-assisted co-electrolysis of glycerol and water for concurrent production of formic acid and hydrogen. Journal of Materials Chemistry A, 2021, 9, 19975-19983.	5.2	18
121	Growth of non-polar ZnO films on a-GaN/r-Al2O3 templates by radio-frequency magnetron sputtering. Journal of Alloys and Compounds, 2010, 489, 519-522.	2.8	17
122	High mobility amorphous InGaZnO thin film transistor with single wall carbon nanotubes enhanced-current path. Applied Physics Letters, 2013, 103, 223108.	1.5	17
123	Efficient enhancement of solar-water-splitting by modified "Z-scheme―structural WO3-W-Si photoelectrodes. Applied Physics Letters, 2014, 105, 143902.	1.5	17
124	Formation of Carbonized Polystyrene Sphere/hemisphere Shell Arrays by Ion Beam Irradiation and Subsequent Annealing or Chloroform Treatment. Scientific Reports, 2015, 5, 17529.	1.6	17
125	Controlling Injection Barriers for Ambipolar 2D Semiconductors via Quasiâ€van der Waals Contacts. Advanced Science, 2019, 6, 1801841.	5.6	17
126	Parallel measurement of conductive and convective thermal transport of micro/nanowires based on Raman mapping. Applied Physics Letters, 2015, 106, .	1.5	16

#	Article	IF	CITATIONS
127	Recent progress in periodic patterning fabricated by self-assembly of colloidal spheres for optical applications. Science China Materials, 2020, 63, 1418-1437.	3.5	16
128	Electronic Coupling of Single Atom and FePS <sub>3</sub> Boosts Water Electrolysis. Energy and Environmental Materials, 2022, 5, 899-905.	7.3	16
129	Controllable Synthesis and Optical Properties of Connected Zinc Oxide Nanoparticles. Chemistry - an Asian Journal, 2010, 5, 315-321.	1.7	15
130	Helium release and amorphization resistance in ion irradiated nanochannel films. Europhysics Letters, 2014, 106, 12001.	0.7	15
131	Significantly enhanced visible light response in single TiO2 nanowire by nitrogen ion implantation. Nanotechnology, 2018, 29, 184005.	1.3	15
132	Construct Fe2+ species and Au particles for significantly enhanced photoelectrochemical performance of α-Fe2O3 by ion implantation. Science China Materials, 2018, 61, 878-886.	3.5	15
133	Recent progress of radiation response in nanostructured tungsten for nuclear application. Tungsten, 2021, 3, 20-37.	2.0	15
134	Facile Fabrication of Ultrafine Hollow Silica and Magnetic Hollow Silica Nanoparticles by a Dual-Templating Approach. Nanoscale Research Letters, 2010, 5, 116-123.	3.1	14
135	Side-to-side alignment of gold nanorods with polarization-free characteristic for highly reproducible surface enhanced Raman scattering. Applied Physics Letters, 2014, 105, 211902.	1.5	14
136	Low Interface Trap Densities and Enhanced Performance of AlGaN/GaN MOS High- Electron Mobility Transistors Using Thermal Oxidized Y <sub>2</sub> O <sub>3</sub> Interlayer. IEEE Electron Device Letters, 2015, 36, 1284-1286.	2.2	14
137	Synthesis and photocatalytic application of trinary structural g-C3N4/Ag/Ag3PO4 composite nanomaterials. Journal of Environmental Chemical Engineering, 2017, 5, 5777-5785.	3.3	14
138	Flexible cation-based threshold selector for resistive switching memory integration. Science China Information Sciences, 2018, 61, 1.	2.7	14
139	Recent progress about 2D metal dichalcogenides: Synthesis and application in photodetectors. Nano Research, 2021, 14, 1819-1839.	5.8	14
140	Fabrication of single-crystal ZnO film by Zn ion implantation and subsequent annealing. Nanotechnology, 2007, 18, 285609.	1.3	13
141	Fabrication and properties of TiO <sub>2</sub> nanofilms on different substrates by a novel and universal method of Ti-ion implantation and subsequent annealing. Nanotechnology, 2013, 24, 255603.	1.3	13
142	Size-dependent radiation tolerance and corrosion resistance in ion irradiated CrN/AlTiN nanofilms. Nuclear Instruments & Methods in Physics Research B, 2015, 342, 137-143.	0.6	13
143	Design of high performance MoS <sub>2</sub> -based non-volatile memory via ion beam defect engineering. 2D Materials, 2019, 6, 034002.	2.0	12
144	In-situ structural evolution of Bi <sub>2</sub> O <sub>3</sub> nanoparticle catalysts for CO <sub>2</sub> electroreduction. International Journal of Extreme Manufacturing, 2022, 4, 035002.	6.3	12

#	Article	IF	CITATIONS
145	Formation of TiO2nanorods by ion irradiation. Journal of Applied Physics, 2014, 115, 184306.	1.1	11
146	Controlled preparation of hollow SnO2@M (M = Au, Ag) heterostructures through template-assist method for enhanced photocatalysis. Colloids and Surfaces A: Physicochemical and Engineering Aspects, 2015, 482, 276-282.	2.3	11
147	Recent progress in the fabrication of SERS substrates based on the arrays of polystyrene nanospheres. Science China: Physics, Mechanics and Astronomy, 2016, 59, 1.	2.0	11
148	Formation of nanoripples on ZnO flat substrates and nanorods by gas cluster ion bombardment. Beilstein Journal of Nanotechnology, 2020, 11, 383-390.	1.5	11
149	Enhanced mechanical property and radiation resistance of reduced graphene oxide/tungsten composite with nacre-like architecture. Composite Structures, 2020, 245, 112361.	3.1	11
150	High performance amorphous ZnMgO/carbon nanotube composite thin-film transistors with a tunable threshold voltage. Nanoscale, 2013, 5, 2830.	2.8	10
151	Structure and Growth Mechanism of V/Ag Multilayers with Different Periodic Thickness Fabricated by Magnetron Sputtering Deposition. Journal of Materials Science and Technology, 2014, 30, 1012-1019.	5.6	10
152	Morphology effect of polythiophene catalysts on photo-degradation of methylene blue. RSC Advances, 2016, 6, 74968-74972.	1.7	10
153	Surfaceâ€Regulated Rhodium–Antimony Nanorods for Nitrogen Fixation. Angewandte Chemie, 2020, 132, 8143-8148.	1.6	10
154	Photo/Bioâ€Electrochemical Systems for Environmental Remediation and Energy Harvesting. ChemSusChem, 2020, 13, 3391-3403.	3.6	10
155	A Highâ€Speed Photodetector Fabricated with Tungstenâ€Doped MoS <sub>2</sub> by Ion Implantation. Advanced Electronic Materials, 2022, 8, .	2.6	10
156	Controlling the growth of ZnO quantum dots embedded in silica by Zn/F sequential ion implantation and subsequent annealing. Nanotechnology, 2008, 19, 155610.	1.3	9
157	Size control and magnetic properties of single layer monodisperse Ni nanoparticles prepared by magnetron sputtering. Journal of Materials Science, 2012, 47, 508-513.	1.7	9
158	Interface Energy Coupling between β-tungsten Nanofilm and Few-layered Graphene. Scientific Reports, 2017, 7, 12213.	1.6	9
159	Enhancing resistance to radiation hardening and radiation thermal conductivity degradation by tungsten/graphene interface engineering. Journal of Nuclear Materials, 2020, 539, 152348.	1.3	9
160	ZnO single-crystal films fabricated by the oxidation of zinc-implanted sapphire. Nanotechnology, 2008, 19, 325604.	1.3	8
161	Synergistic effect of V/N codoping by ion implantation on the electronic and optical properties of TiO2. Journal of Applied Physics, 2014, 115, 143106.	1.1	8
162	Gate dielectric ion implantation to modulate the threshold voltage of In2O3 nanowire field effect transistors. Applied Physics Letters, 2016, 109, .	1.5	8

#	Article	IF	CITATIONS
163	Sputtering of silicon nanopowders by an argon cluster ion beam. Beilstein Journal of Nanotechnology, 2019, 10, 135-143.	1.5	8
164	Exploring and suppressing the kink effect of black phosphorus field-effect transistors operating in the saturation regime. Nanoscale, 2019, 11, 10420-10428.	2.8	8
165	High performance perovskite LEDs via SPR and enhanced hole injection by incorporated MoS <sub>2</sub> . Journal Physics D: Applied Physics, 2021, 54, 214002.	1.3	8
166	2D Heterostructure of Bi <sub>2</sub> O <sub>2</sub> Se/Bi <sub>2</sub> SeO <i><sub>x</sub></i> Nanosheet for Resistive Random Access Memory. Advanced Electronic Materials, 2022, 8, .	2.6	8
167	Fabrication and optical properties of controlled Ag nanostructures for plasmonic applications. Journal of Applied Physics, 2013, 114, 083523.	1.1	7
168	Spindle-Like <i>α</i> -Fe <sub>2</sub> O <sub>3</sub> Embedded with TiO <sub>2</sub> Nanocrystalline: Ion Implantation Preparation and Enhanced Magnetic Properties. Journal of Nanoscience and Nanotechnology, 2013, 13, 5428-5433.	0.9	7
169	Tunable Electrical Properties in High-Valent Transition-Metal-Doped ZnO Thin-Film Transistors. IEEE Electron Device Letters, 2014, 35, 759-761.	2.2	7
170	Anionic Dopant Delocalization through pâ€Band Modulation to Endow Metal Oxides with Enhanced Visibleâ€Light Photoactivity. Angewandte Chemie, 2019, 131, 16813-16820.	1.6	7
171	Fabrication of Ag nanoclusters in single-crystal MgO by high-energy ion implantation. Physica E: Low-Dimensional Systems and Nanostructures, 2008, 40, 705-708.	1.3	6
172	Energy dependence on formation of TiO2 nanofilms by Ti ion implantation and annealing. Materials Research Bulletin, 2014, 51, 376-380.	2.7	6
173	Co2P Nanoparticles Wrapped in Amorphous Porous Carbon as an Efficient and Stable Catalyst for Water Oxidation. Frontiers in Chemistry, 2018, 6, 580.	1.8	6
174	Regulation of Two-Dimensional Lattice Deformation Recovery. IScience, 2019, 13, 277-283.	1.9	6
175	Intrinsic defects of nonprecious metal electrocatalysts for energy conversion: Synthesis, advanced characterization, and fundamentals. ChemPhysMater, 2022, 1, 155-182.	1.4	6
176	Controllable Synthesis of TiO2 Submicrospheres with Smooth or Rough Surface. Chemistry Letters, 2010, 39, 684-685.	0.7	5
177	Influence of annealing temperature on the properties of TiO2 films annealed by ex situ and in situ TEM. Journal Wuhan University of Technology, Materials Science Edition, 2012, 27, 1014-1019.	0.4	5
178	A Novel Way to Fabricate Superhydrophilic and Antibacterial TiO2Nanofilms on Glass by Ion Implantation and Subsequent Annealing. Japanese Journal of Applied Physics, 2013, 52, 100207.	0.8	5
179	Fabrication of TiO <sub>2</sub> -based composite films by sequential ion implantation and subsequent annealing. Materials Research Express, 2014, 1, 025703.	0.8	5
180	Fabrication of highly homogeneous surface-enhanced Raman scattering substrates using Ag ion implantation. Journal of Physics Condensed Matter, 2016, 28, 254003.	0.7	5

#	Article	IF	CITATIONS
181	Controllable synthesis of Au@SnO <sub>2</sub> core–shell nanohybrids with enhanced photocatalytic activities. Materials Research Express, 2017, 4, 055502.	0.8	5
182	Small Al cluster ion implantation into Si and 4H‧iC. Rapid Communications in Mass Spectrometry, 2019, 33, 1449-1454.	0.7	5
183	Two-dimensional PtPb-PbS heterostructure enables improved kinetics and highlighted bifunctional antipoisoning for methanol electrooxidation. Science China Chemistry, 2022, 65, 1112-1121.	4.2	5
184	Antibacterial Silver-Containing Silica Glass Prepared by Ion Implantation. Journal of Nanoscience and Nanotechnology, 2010, 10, 6424-6427.	0.9	4
185	Broadband light generation from Au–Al <sub>2</sub> O <sub>3</sub> –Al sub-10 nm plasmonic gap structures. Journal of Materials Chemistry C, 2017, 5, 6771-6776.	2.7	4
186	Resistive Switching: Breaking the Current-Retention Dilemma in Cation-Based Resistive Switching Devices Utilizing Graphene with Controlled Defects (Adv. Mater. 14/2018). Advanced Materials, 2018, 30, 1870100.	11.1	4
187	Modulating the filament rupture degree of threshold switching device for self-selective and low-current nonvolatile memory application. Nanotechnology, 2020, 31, 144002.	1.3	4
188	Low Surface Accessible Area NanoCoral TiO <sub>2</sub> for the Reduction of Foreign Body Reaction During Implantation. Advanced Healthcare Materials, 2022, 11, e2200382.	3.9	4
189	Plasmonic Polycrystals within Microbowl Arrays. Advanced Optical Materials, 2022, 10, .	3.6	4
190	The use of electron backscatter diffraction to measure the elastic strain fields in a misfit dislocation-free InGaAsP/InP heterostructure. Journal Physics D: Applied Physics, 2007, 40, 7302-7305.	1.3	3
191	Formation of metal nanoparticles in silica by the sequential implantation of Ag and Cu. Applied Physics A: Materials Science and Processing, 2007, 89, 681-684.	1.1	3
192	Heteroepitaxial growth and structural characterization of rutile TiO2 thin films on GaN (0001) templates prepared by pulsed laser deposition. Nuclear Instruments & Methods in Physics Research B, 2013, 307, 477-481.	0.6	3
193	Transparent megahertz circuits from solution-processed composite thin films. Nanoscale, 2016, 8, 7978-7983.	2.8	3
194	Fabrication of TiO2Nanofilm Photoelectrodes on Ti Foil by Ti Ion Implantation and Subsequent Annealing. Advances in Condensed Matter Physics, 2014, 2014, 1-7.	0.4	1
195	Graphene: Confining Cation Injection to Enhance CBRAM Performance by Nanopore Graphene Layer (Small 35/2017). Small, 2017, 13, .	5.2	1
196	Rapid and sensitive detection of 4-ethylbenzaldehyde by a plasmonic nose. Journal Physics D: Applied Physics, 2021, 54, 255306.	1.3	1
197	One-pot Reaction To Synthesis And Characterization Of Two-stage Zinc Oxide Hexagonal Microprism On Nickel Thin Films. Advanced Materials Letters, 2013, 4, 610-614.	0.3	1
198	Field-emission SEM characterization of novel ZnO thin films grown by magnetron sputtering on the		0

different substrates. , 2009, , .

#	Article	IF	CITATIONS
199	Fabrication and evolution of nanostructure in Al2O3 single crystals by Zn+ ion implantation and thermal annealing. Vacuum, 2013, 89, 132-135.	1.6	0
200	Near Infrared Neuromodulation: Precise Modulation of Gold Nanorods for Protecting against Malignant Ventricular Arrhythmias via Nearâ€Infrared Neuromodulation (Adv. Funct. Mater. 36/2019). Advanced Functional Materials, 2019, 29, 1970251.	7.8	0
201	Innenrücktitelbild: Active Electron Density Modulation of Co <sub>3</sub> O <sub>4</sub> â€Based Catalysts Enhances their Oxygen Evolution Performance (Angew. Chem. 17/2020). Angewandte Chemie, 2020, 132, 7003-7003.	1.6	0
202	Strong Penetrationâ€Induced Effective Photothermal Therapy by Exosomeâ€Mediated Black Phosphorus Quantum Dots (Small 49/2021). Small, 2021, 17, .	5.2	0